

# Journal of Materials Chemistry B

Accepted Manuscript



This article can be cited before page numbers have been issued, to do this please use: L. Xu, M. Zhao, Y. Yang, Y. Liang, C. Sun, W. Gao, S. Li, B. He and Y. Pu, *J. Mater. Chem. B*, 2017, DOI: 10.1039/C7TB02359F.



This is an Accepted Manuscript, which has been through the Royal Society of Chemistry peer review process and has been accepted for publication.

Accepted Manuscripts are published online shortly after acceptance, before technical editing, formatting and proof reading. Using this free service, authors can make their results available to the community, in citable form, before we publish the edited article. We will replace this Accepted Manuscript with the edited and formatted Advance Article as soon as it is available.

You can find more information about Accepted Manuscripts in the [author guidelines](#).

Please note that technical editing may introduce minor changes to the text and/or graphics, which may alter content. The journal's standard [Terms & Conditions](#) and the ethical guidelines, outlined in our [author and reviewer resource centre](#), still apply. In no event shall the Royal Society of Chemistry be held responsible for any errors or omissions in this Accepted Manuscript or any consequences arising from the use of any information it contains.



Journal Name

ARTICLE

## A reactive oxygen species (ROS)-responsive low molecular weight gel co-loaded with doxorubicin and Zn(II) phthalocyanine tetrasulfonic acid for combined chemo-photodynamic therapy

Long Xu<sup>a,b</sup>, Mingying Zhao<sup>c</sup>, Yidi Yang<sup>a</sup>, Yan Liang<sup>d</sup>, Changzhen Sun<sup>a</sup>, Wenxia Gao<sup>\*b</sup>, Sai Li<sup>c</sup>, Bin He<sup>a</sup>, and Yuji Pu<sup>\*a</sup>

Received 00th January 20xx,  
Accepted 00th January 20xx

DOI: 10.1039/x0xx00000x

www.rsc.org/

Low molecular weight gels (LMWGs) have significant advantages in drug delivery such as high drug loading capacity, *in situ* delivery of drug to the lesion site, sustaining drug release with excellent bioavailability, and minimized side effects. Here, we synthesized a reactive oxygen species (ROS)-responsive gelator to prepare an injectable gel. Anticancer drug doxorubicin hydrochloride (DOX) and photosensitizer Zn(II) phthalocyanine tetrasulfonic acid (ZnPCS<sub>4</sub>) were loaded in the gel for combined chemo-photodynamic therapy. The ROS-responsive gelator was characterized by proton nuclear magnetic resonance (<sup>1</sup>H NMR) and the morphology of gels were investigated by scanning electron microscopy (SEM). The rheological properties and destroy-recovery capability of both blank and drug-loaded gels were studied. The cytotoxicity of LMWGs against 3T3 fibroblasts and 4T1 breast cancer cells were tested. The *in vitro* drug release of both drugs were studied and the *in vivo* anticancer activities of DOX-ZnPCS<sub>4</sub>-coloaded LMWGs were investigated in tumor-bearing mice. The results revealed that the injectable DOX-ZnPCS<sub>4</sub>-coloaded LMWGs had excellent anti-tumor efficacy and played a coordinated treatment efficacy.

### Introduction

Chemotherapy, a very important cancer therapy mode, has been widely used in the clinical treatment of various cancers.<sup>1,2</sup> Small-molecule chemotherapeutics has obvious limits, such as systemic toxicity due to lack of specific selectivity to distinguish healthy and cancer cell and short blood circulation because of rapid clearance by endothelial reticular system (RES).<sup>3</sup> Nanoparticulate drug delivery systems (NDDSs) have been developed to prolong the blood circulation and reduce side effects by affecting the bio-distribution and tuning the drug release behaviours.<sup>4-7</sup> NDDS is generally administrated by intravenous injection that may lead to drug leakage during long blood circulation and toxicity to normal organs.<sup>8,9</sup> The localized drug delivery strategy provides an alternative way for cancer therapy, which directly delivers the chemotherapeutics to the lesion site and thus minimized toxicity to other organs.<sup>10,11</sup> One approach is to exploit drug-loaded injectable

gels to realize localized drug delivery by intratumor injection.<sup>10,12-14</sup> Specifically, low molecular weight gels (LMWGs) have aroused extensive interest in various biomedical applications such as drug delivery, 3D-cell culture, enzyme immobilization, and induction of mesenchymal stromal cells (MSC) differentiation.<sup>15-20</sup> LMWGs, as an anticancer drug delivery system, have great advantages and application prospects: (1) They are biocompatible, non-toxic, and biodegradable due to low toxicity of low molecular weight gelators; (2) They display high drug loading contents; (3) Drug-loaded LMWGs could be administrated by intratumor injection, which directly delivers chemotherapeutic drugs to tumor sites and thus lowers the toxicity to normal organs; (4) Most importantly, the drug-loaded gels, not limited to LMWGs, can sustain drug release by stimuli-responsive degradation and maintain an effective therapeutic concentration.<sup>17,21-23</sup> Many research groups had employed LMWGs for efficient tumor inhibition. For example, Barthélémy et al. investigated the influence of cation on hydrogel and provided a paradigm for *in vivo* sustained drug delivery.<sup>24</sup> Our group developed a phenylboronic acid-based LMWG for efficient local chemotherapy by loading anticancer drug doxorubicin.<sup>25,26</sup>

Different from chemotherapy, photodynamic therapy (PDT), an externally available treatment modality for tumor treatment, employs singlet oxygen (SO) or reactive oxygen species (ROS) generated by photosensitizers (PS) under light irradiation to kill cancer cells.<sup>27,28</sup> The lesion is selectively illuminated with light after administration of PS and cytotoxic ROS are generated, leading to cell death and tissue

<sup>a</sup> National Engineering Research Center for Biomaterials, Sichuan University, Chengdu 610064, China

<sup>b</sup> College of Chemistry & Materials Engineering, Wenzhou University, Wenzhou 325027, China

<sup>c</sup> School of Chemical Engineering, Sichuan University, Chengdu 610065, China

<sup>d</sup> Department of Pharmaceutics, School of Pharmacy, Qingdao University, Qingdao 266021, China

\* Corresponding authors, E-mail: wenxiag@wzu.edu.cn; yjpu@scu.edu.cn

† Electronic Supplementary Information (ESI) available: Characterization of gel precursors, rheological properties of gels formed by control gelators, *in vitro* drug release, and histological analysis of organs of mice treated by control gels. See DOI: 10.1039/x0xx00000x

destruction. Porphyrin and its derivatives have been widely used as PS for PDT.<sup>29,30</sup> Specifically, nanoparticle-based PDT has been developed and shown encouraging results *in vitro* and *in vivo*.<sup>31</sup> Compared with normal tissues, tumor tissue has a more acidic microenvironment and higher concentration of ROS.<sup>32–34</sup> Many ROS-responsive drug delivery systems, mainly containing ROS-cleavable thioketal and thioether bonds, have shown good anticancer effect both *in vitro* and *in vivo*.<sup>35,36</sup>

In this study, a LWMG with ROS-responsive property was designed for combined local chemo-photodynamic therapy. A low molecular weight gelator containing thioketal was designed and synthesized (Scheme 1), and the resulting gel was used for loading chemotherapeutics doxorubicin hydrochloride (DOX) and photosensitizer Zn(II) phthalocyanine tetrasulfonic acid (ZnPCS<sub>4</sub>) to form DOX-ZnPCS<sub>4</sub>-coloaded LWMGs. A control gelator without thioketal bond was also designed and its blank gel and drug-loaded gels were used as control (Scheme 1). In our hypothesis, after intratumor injection of the DOX-ZnPCS<sub>4</sub>-coloaded LWMG, ROS generated by ZnPCS<sub>4</sub> under light irradiation would accelerate the degradation of ROS-responsive LWMG, releasing DOX and ZnPCS<sub>4</sub> for combined chemotherapy and photodynamic therapy (Scheme 2). This dual modal therapy is expected to display synergistic effect for cancer inhibition.<sup>37</sup> The *in vitro* ROS-responsive, rheological property, and drug release of these gels were investigated. The *in vitro* cytotoxicity of gels against mouse fibroblasts NIH/3T3 and 4T1 breast cancer cells was tested. The *in vivo* antitumor efficiencies of these gels were studied.

## Experimental

### Materials

All chemical reagents used in this study were commercially available and chemically pure. L-Phenylalanine methyl ester hydrochloride, 1,1'-carbonyldiimidazole (CDI), sebacoyl chloride, and thiazolyl blue (MTT) were purchased from the Saen chemical technology (Shanghai) Co. Ltd. 3-Mercaptopropionic acid was purchased from Aladdin Bio-Chem technology (Shanghai) Co. Ltd. N, N-Diisopropylethylamine (DIEA) was purchased from Asta Tech (Chengdu) Biopharm. Co. Ltd. Zn(II) Phthalocyanine tetrasulfonic acid (ZnPCS<sub>4</sub>) was purchased from J&K Scientific Ltd. Doxorubicin hydrochloride (DOX) was purchased from Zhejiang Hisun Pharmaceutical. Poly(ethylene glycol) (PEG, *M<sub>w</sub>* = 200 g/mol), *p*-hydroxybenzaldehyde, hydrazine hydrate (80%), and all solvents were purchased from Chengdu Kelong Chemical Co. (China) without further purification prior to use. Dulbecco's modified Eagle's medium (DMEM), 100 × mycillin, and fetal bovine serum (FBS) were purchased from Gibco Inc.

### Characterizations

All the compounds were characterized by proton nuclear magnetic resonance (<sup>1</sup>H NMR), which were performed on a Bruker Avance II NMR spectrometer at 400 MHz using tetramethylsilane as the internal standard. Scanning electron microscope (SEM, S4800, Hitachi Ltd, Tokyo, Japan) was employed to observe the

morphology of gel. The rheological property was studied on a rheometer (Discovery DHR-2, TA, American).

### Synthesis of the ROS-responsive gelator

The synthetic scheme of ROS-responsive gelator is shown in Scheme 1.

**Synthesis of ROS-cleavable neotype thioketal (TK).** A mixture of 3-mercaptopropionic acid (11.44 g, 108.02 mmol) and *p*-hydroxybenzaldehyde (6.0 g, 49.1 mmol) were dissolved in ethyl acetate. Catalytic amount of trifluoroacetic acid were added and the solution was stirred at room temperature (RT). The reaction was monitored by thin layer chromatography. When *p*-hydroxybenzaldehyde was exhausted, the solvents were removed and the crude product was washed by CH<sub>2</sub>Cl<sub>2</sub> and cold water for several times. White product was obtained after drying.

**Synthesis of Phe-TK-Phe.** L-Phenylalanine methyl ester hydrochloride (4.48 g, 22 mmol) was dissolved in dry CH<sub>2</sub>Cl<sub>2</sub> (50 mL). DIEA (2.84 g, 22 mmol) was added dropwise to the solution at an ice bath and stirred for 10 min. In a separate flask, 3,3'-(((4-hydroxyphenyl)methylene)bis(sulfanediyl))dipropanoic acid (3.16 g, 10 mmol) and CDI (3.57 g, 22 mmol) were dissolved in 30 mL dry CH<sub>2</sub>Cl<sub>2</sub> and the solution was stirred at RT for 30 min. The activated acid solution was added dropwise to the mixture of L-phenylalanine methyl ester hydrochloride at an ice bath followed by stirring under N<sub>2</sub> atmosphere for 24 h. The mixed solution was washed with 1 M HCl solution, saturated NaHCO<sub>3</sub> solution and NaCl solution, and dried with anhydrous sodium sulfate. The solvents were removed by rotary evaporation and purified by column chromatography (petroleum ether and ethyl acetate, v/v, 1:2) to obtain the product.

**Synthesis of ROS-responsive and control gelator.** A mixture of Phe-TK-Phe (3.19 g, 5 mmol) and hydrazine hydrate (2 mL) was dissolved in CH<sub>2</sub>Cl<sub>2</sub> and methanol (40 mL, v/v, 1:1). The mixture was then stirred under N<sub>2</sub> atmosphere for 24 h. The mixture was filtrated and washed with dichloromethane for several times. The gelator was obtained after vacuum drying. The control gelator was synthesized similarly (Scheme 1).

### Gel preparation

A given mass of gelator in 1 mL of PEG200 and H<sub>2</sub>O (1:1, v/v) was placed in a flask fitted with a reflux condenser and heated until complete dissolution of the gelator. When cooled to RT, the solution was transferred into a closed glass vial. The gel was obtained by cooling to RT to gelate the solvent. The critical gelation concentration (CGC) was determined by measuring the minimum amount of gelator required for the formation of a stable gel at 37 °C. The SEM images were obtained from gels prepared in ethanol, which were dried under reduced pressure by oil pump at RT.

Drug-loaded gel was prepared by dissolving the payload (DOX and/or ZnPCS<sub>4</sub>) and gelator in PEG200 and H<sub>2</sub>O (1:1, v/v) under heat and then cooling the solution to RT to form DOX-loaded, ZnPCS<sub>4</sub>-loaded, and DOX-ZnPCS<sub>4</sub>-coloaded gels. The concentration of gelator and payload was 30 and 2 mg/mL, respectively. The blank, DOX-loaded, ZnPCS<sub>4</sub>-loaded, and DOX-

ZnPCS<sub>4</sub>-coloaded gels were abbreviated as G1, G2, G3, and G4. The drug-loaded control gel was prepared similarly, except the concentration of control gelator was 10 mg/mL. The blank, DOX-loaded, ZnPCS<sub>4</sub>-loaded, and DOX-ZnPCS<sub>4</sub>-coloaded control gels were abbreviated as G1\*, G2\*, G3\*, and G4\*.

#### **In vitro degradation of gelator under ROS condition**

The degradation of gelator under ROS condition was investigated by <sup>1</sup>H NMR. Gelator (10 mg) was incubated in 4 mL of fresh aqueous solution with 400 mM H<sub>2</sub>O<sub>2</sub> and 3.2 μM CuCl<sub>2</sub> and 2 mL acetone for 48 h. The solution was lyophilized and the <sup>1</sup>H NMR spectrum of the obtained mixture was studied.

#### **Rheological measurements**

In order to investigate the viscoelastic properties of the blank and drug-loaded gels, the storage modulus (*G'*), loss modulus (*G''*), and dynamic complex viscosity (*η\**) of gels were measured.<sup>18,38–40</sup> The angular frequency (*ω*) applied to the gel and drug-loaded gel samples increased from 0.1 to 100 rad/s with a strain of 1.0%. In order to obtain more information of the gel network structure, the dynamic strain sweep and dynamic time sweep was carried out. The dynamic strain sweep was used to destroy the gel network structure, then the dynamic time sweep was used to study the recovery properties of the gel. In details, after the gel was entirely formed, the strain was applied to the gel with an increase from 0.01 to 50% (10 rad/s and 25 °C), then the dynamic time sweep was carried out with the strain 1% (1 rad/s and 25 °C).

#### **Cytotoxicity test**

Mouse fibroblasts NIH/3T3 and 4T1 breast cancer cells were used to evaluate the biocompatibility and toxicity of the gels. The cytotoxicity of gel was carried out by testing the cytotoxicity of gelator according to International Organization for Standardization (ISO) tests (ISO 10993-5).<sup>25</sup> The gelators with different concentration (0.5, 1, 5, 10, 20, and 30 mg/mL) were added to complete culture medium at 37 °C and incubated for 24 h, then extracts were filtered and added to NIH/3T3 cells and 4T1 breast cancer cells for additional 48 h. The culture medium was removed and the wells were washed with PBS (pH7.4). MTT in blank culture medium was added to each well. Subsequently, the cells were incubated for additional 3 h. The culture medium was removed and DMSO (100 μL) was added into each well. The cell viability was determined by measuring the absorption at 490 nm using a microplate reader (Thermo Scientific MK3).

#### **In vitro drug release**

The DOX-ZnPCS<sub>4</sub>-coloaded gel and control gel were prepared according to the aforementioned method. Subsequently, 1 mL drug-coloaded gel in 4 mL threaded bottle was transferred into a threaded bottle with 25 mL PBS buffer solutions. Hydrogen peroxide (H<sub>2</sub>O<sub>2</sub>, 500 mM) was used to provide ROS.<sup>41,42</sup> The threaded bottle was incubated in a constant temperature water bath oscillator at 37 °C immediately. At a predetermined time interval, 1 mL PBS was taken out and 1 mL fresh PBS was added. The released DOX and ZnPCS<sub>4</sub> were determined by a fluorescence detector with excitation wavelength at 480 and

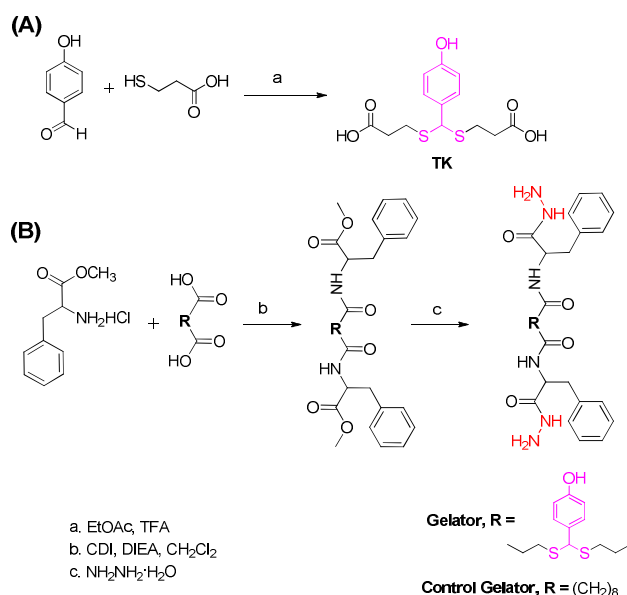
315 nm and emission wavelength at 560 and 355 nm, respectively. The release experiments were conducted in three parallel experiments.

#### **In vivo antitumor activity**

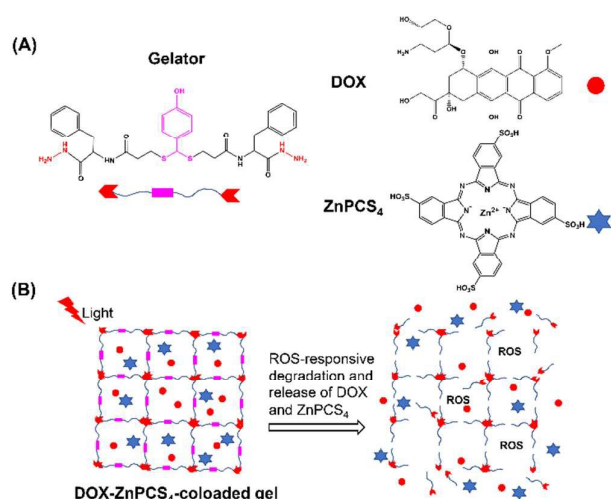
All animal experiments were performed in compliance with the Animal Management Rules of the Ministry of Health of the People's Republic of China (Document no. 55, 2001) and the institutional guidelines. The experiments were approved by Sichuan University Animal Care and Use Committee. Male BALB/c mice (body weight: 18–22 g) were purchased from Dashuo (Chengdu) Biotechnology Co. Ltd. The tumor-bearing mice model was established by inoculated the 4T1 breast cancer cells into right flank subcutaneously of BALB/c mice. After the inoculated tumor volume reached 100–200 mm<sup>3</sup>, the mice were randomly divided into 11 groups. Six groups were treated with the formulations of G1, G3, G4, G1\*, G3\*, and G4\*. All these groups were irradiated for 5 min with a 660 nm (100 W) laser after 30 min of intratumor injection (L+). The other groups were treated with the formulations of G2, G3, G2\*, G3\*, and saline without irradiation (L–). All groups were injected for four times at a 3-day interval with a drug dose of 5 mg/kg. The body weights of mice and the tumor volumes were measured at a 3-day interval. The behaviours of mice were determined by the animal healthcare technicians. Tumor volumes were calculated using the formula  $V = (a \times (b \times b))/2$ , with a the largest and b the smallest diameters. All the dates of tumor volumes and body weight were expressed as relative values, compared to the tumor volume and body weight determined on the first day of therapy. After the experiment, all of the animals were euthanized and sacrificed, and the heart, liver, spleen, lung, kidney, and tumor were separated and washed with PBS, and fixed by 4% formaldehyde. Subsequently, all the organs and tumor were dealt with the histopathological procedures. Hematoxylin and eosin (H&E) staining and the terminal deoxynucleotidyl transferase-mediated dUTP nick end labeling (TUNEL) assay were taken to evaluate the acute toxicity and the apoptosis of cancer cells.

## **Results and discussion**

### **Synthesis and characterization of gelator**



**Scheme 1.** The synthetic scheme of TK (A), thioketal containing and control gelators (B).



**Scheme 2.** (A) Chemical structures of thioketal containing gelator, DOX, and ZnPCS<sub>4</sub>. (B) The illustration of ROS-responsive degradation of DOX-ZnPCS<sub>4</sub>-co-loaded gel and the release of DOX and ZnPCS<sub>4</sub> for combined chemophotodynamic therapy.

The thioketal containing and control gelators were synthesized (Scheme 1) and characterized by <sup>1</sup>H NMR. For the ROS-responsive gelator, the 3,3'-(p-hydroxybenzylidene)dithiodipropionic acid (TK) was successfully obtained through the aldolization, which has a methyne characteristic peak appeared at  $\delta$  5.15 ppm (Fig. S1A). The L-phenylalanine methyl ester hydrochloride was conjugated to TK through amide condensation reaction, followed by a reaction with hydrazine hydrate to obtain thioketal containing gelator. The successful synthesis of ROS-responsive gelator was proved by

the disappearance of the characteristic peak of -OCH<sub>3</sub> ( $\delta$  3.70 ppm, Fig. S1C). The control gelator was similarly synthesized and characterized by <sup>1</sup>H NMR in Fig. S2.

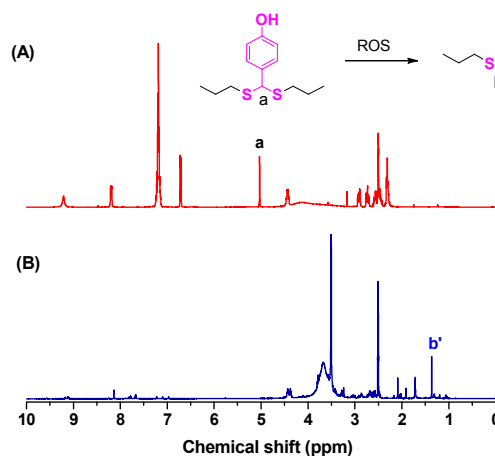


**Fig. 1.** <sup>1</sup>H NMR spectra of gelator before (A) and after (B) treatment of ROS stimulus where Fenton reagent was used to mimic ROS conditions in CDCl<sub>3</sub> and DMSO-*d*<sub>6</sub>, respectively. The inset showed the chemical change of thioketal to thiol in the presence of ROS.

In order to verify the ROS-responsiveness of the thioketal containing gelator, the gelator was incubated with fresh Fenton reagent that mimics the ROS condition. The obtained product was characterized by <sup>1</sup>H NMR.<sup>43</sup> After the incubation in ROS condition, the thioketal characteristic peak ( $\delta$  = 5.03 ppm, peak a in Fig. 1A) of gelator disappeared and a new peak at 1.38 ppm (peak b in Fig. 1B) emerged, which was ascribed to the proton of thiol group, suggesting the ROS-responsiveness of thioketal containing gelator. However, no change was observed in the <sup>1</sup>H NMR spectra of control gel before and after treatment of ROS (Fig. S3), suggesting no response to ROS.

#### Gel characterizations

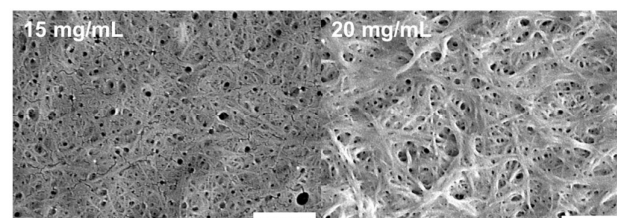


**Fig. 2.** The SEM images of xerogel prepared in ethanol with a gelator concentration of 15 and 20 mg/mL; the bar was 500 nm.

The critical gel concentrations (CGCs) of the two gelators were tested in different solvents at 37 °C; the results were shown in Table S1. Both ROS-responsive gelator and control gelator can facilely form gels in ethanol or methanol with a CGC of 10 mg/mL. The microtopography of ROS-responsive xerogel prepared in ethanol was characterized by SEM and typical network structure was observed (Fig. 2).

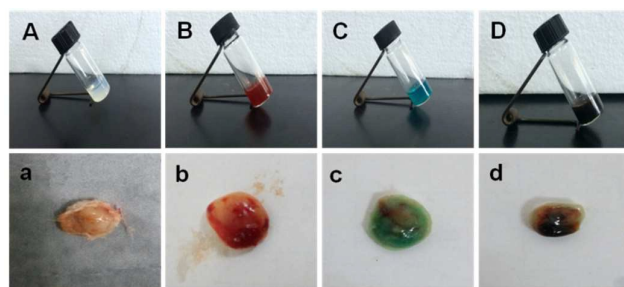


**Fig. 3.** The images of various ROS-responsive gels (top row) and tumors (down row) treated with these gels. Gels: blank gel (A, a); DOX-loaded gel (B, b); ZnPCS<sub>4</sub>-loaded gel (C, c); and DOX-ZnPCS<sub>4</sub>-coloaded gel (D, d).

Besides, both gelators can form gels in PEG200-H<sub>2</sub>O (5:1–1:1, v/v) mixed solution (Table S1). The biocompatible and nontoxic PEG200 was added to deionized water to improve the solubility of gelator and facilitate gel formation.<sup>18, 25</sup> The thiolketal containing gelator showed a higher CGC in PEG200-H<sub>2</sub>O of 30 mg/mL than that of control gelator (5 mg/mL). Moreover, the gel was demonstrated to have an excellent capability to load anticancer drug doxorubicin hydrochloride (DOX) and photosensitizer Zn(II) phthalocyanine tetrasulfonic acid (ZnPCS<sub>4</sub>) alone or both (structures of DOX and ZnPCS<sub>4</sub> were shown in Scheme 2A). The drug loading contents of both DOX and ZnPCS<sub>4</sub> were 6.25% in these gels. The typical blank gel (G1), DOX-loaded (G2), ZnPCS<sub>4</sub>-loaded (G3), and DOX-ZnPCS<sub>4</sub>-coloaded gels (G4) formed by thiolketal containing gelator were shown in Fig. 3A–3D. For the dispersion form of drug molecules, when the drug molecules were dissolved in aqueous solution, the crystal structure was destroyed to be soluble in the solvent, and no crystallization was observed in the process of drug-loaded gel formation or during the storage period. Therefore, DOX and ZnPCS<sub>4</sub> were molecularly dispersed in the gel network and crystal was hard to form because of dispersion in the gel network. Control gels were prepared similarly and the drug loading contents of DOX and ZnPCS<sub>4</sub> were 9.09%.

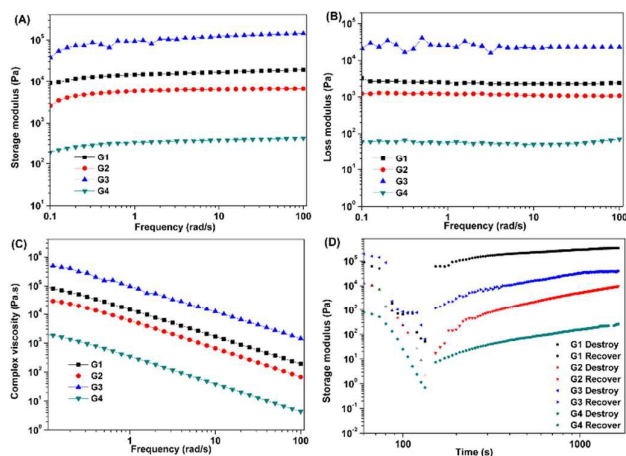


**Fig. 4.** The rheological properties of ROS-responsive blank gel and drug-loaded gels: storage modulus (A) and loss modulus (B) as a

function of angular frequency of the gels; (C) dynamic complex viscosity as a function of angular frequency for the gels; (D) destroy and recovery of the gels.

The viscoelastic properties of these gels (G1–G4) were investigated. All the samples used for rheological test were real gels, which were confirmed by the fact that the storage modulus ( $G'$ ) of gels was higher than their corresponding loss modulus ( $G''$ ) (Fig. 4A and 4B). The dynamic modulus decreased with the order of  $G3 > G1 > G2 > G4$ , implying that G3 (ZnPCS<sub>4</sub>-loaded gel) and G4 (DOX-ZnPCS<sub>4</sub>-coloaded gel) had the biggest and smallest mechanical strength, respectively. The enhanced mechanical strength of G3 might be ascribed to the supramolecular interactions of ZnPCS<sub>4</sub> and gelator, where aromatic structures and opposite charges (-NHNH<sub>2</sub> and -SO<sub>3</sub>H) might induce  $\pi$ - $\pi$  interactions and electrostatic interactions, respectively. Although DOX has an aromatic structure, the amine group in DOX might result in electrostatic repulsion between DOX and gelator, reducing the mechanical strength. The G4, however, showed the lowest mechanical strength, which might be due to its higher drug loading content (the total drug loading contents for G2, G3, and G4 were 6.25%, 6.25%, and 12.5%, respectively) that somehow disrupt the tacticity and lead to more disorder of gel network, resulting lower mechanical strength. The frequency dependence of dynamic complex viscosity ( $\eta^*$ ) indicated that all the gels had a shear-thinning behaviour (Fig. 4C). As the dynamic strain and time sweep results (Fig. 4D) showed, the network structure of gel was destroyed after increasing strain and recovered after the removal of the strain. This result was owing to the intrinsic dynamic and reversible supramolecular interactions between gelators, which could respond to the external strain.<sup>44,45</sup> The shear-thinning property and excellent destroy-recover ability make supramolecular drug-loaded gels potential candidates for intratumor injection.<sup>46</sup> The rheological data of control gel and its drug-loaded gel were also tested and similar rheological results were observed (Fig. S4).

### Cytotoxicity

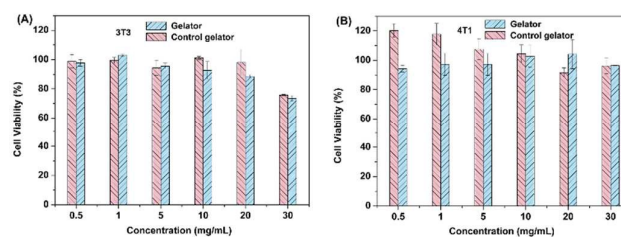


**Fig. 5.** The cytotoxicity of ROS-responsive and control gels incubated with NIH/3T3 fibroblasts (A) and 4T1 breast cancer cells (B).

The biocompatibility of ROS-responsive gels and control gels was evaluated by MTT assay using NIH/3T3 fibroblasts and 4T1 breast cancer cells. As shown in Fig. 5B, the cell viabilities of 4T1 cells were higher than 90% for both gelator extracts even at a high gelator concentration of 30 mg/mL. Neglectable cytotoxicity against NIH/3T3 fibroblasts cells was observed when gelator concentration

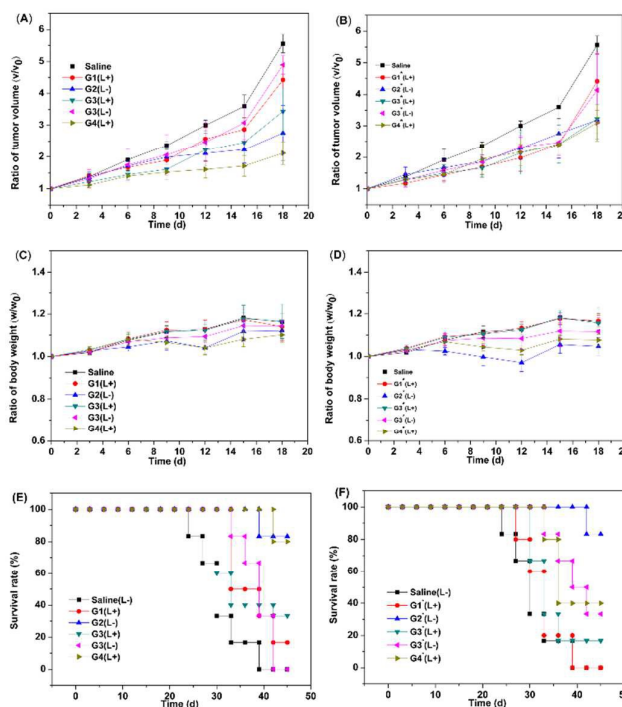
## ARTICLE

was no more than 20 mg/mL (Fig. 5A). These results showed that the gels showed low cytotoxicity and good biocompatibility.

**In vitro drug release**

The *in vitro* release of DOX-ZnPCS<sub>4</sub>-coloaded gel and DOX-ZnPCS<sub>4</sub>-coloaded control gel in PBS (pH 7.4), PBS with 500 mM H<sub>2</sub>O<sub>2</sub>, and PBS with 500 mM H<sub>2</sub>O<sub>2</sub> and irradiation was studied. Hydrogen peroxide (H<sub>2</sub>O<sub>2</sub>) was used to provide ROS. We found that the fluorescence intensity of ZnPCS<sub>4</sub> was not proportional to the concentration of the ZnPCS<sub>4</sub> (Fig. S5) even though the concentration was as low as  $1.22 \times 10^{-4}$  μg/mL, and fluorescence quenches at a high concentration of ZnPCS<sub>4</sub>. Therefore, we cannot detect the amount of released ZnPCS<sub>4</sub> by fluorescence spectroscopy. Although the quantitative release was hard to obtain, we can qualitatively evaluate the release of the ZnPCS<sub>4</sub> by its color (Fig. S6). The green color of ZnPCS<sub>4</sub> in the release medium of DOX-ZnPCS<sub>4</sub>-coloaded gel treated with ROS condition (Fig. S6e) was obviously darker than that of DOX-ZnPCS<sub>4</sub>-coloaded control gel (no obvious green color was observed, Fig. S6b), demonstrating its ROS-responsive release behavior. Moreover, the greenest color of the release medium was observed in the DOX-ZnPCS<sub>4</sub>-coloaded gel treated with ROS condition and light irradiation (Fig. S6f), demonstrating the most release of ZnPCS<sub>4</sub> in all groups. This result was ascribed to its light-activated ROS generation *in situ*, which simultaneously triggered the cleavage of thioketal bond and gel degradation, and the acceleration of drug release.

Unexpectedly, we did not observe the typical emission peak of DOX (560 nm) under ROS condition by fluorescence spectroscopy. We hypothesize that the H<sub>2</sub>O<sub>2</sub> could oxidize the phenolic hydroxyl groups on the anthraquinone ring of DOX, then the conjugated structure is destroyed and leads to fluorescence quenching of DOX. We then tested the fluorescence emission of DOX in the presence of H<sub>2</sub>O<sub>2</sub>. The PBS (pH 7.4) solution of DOX was incubated with different concentrations of H<sub>2</sub>O<sub>2</sub> (0, 50, 150, and 250 mM) for different times (1, 3, and 6 h). The more fluorescence quenching was observed when the solution was treated with higher concentration of H<sub>2</sub>O<sub>2</sub> or longer incubation time (Fig. S7). Therefore, it is inaccurate to quantify the release of DOX by fluorescence spectroscopy in the presence of H<sub>2</sub>O<sub>2</sub>. Taking together, light-activated rapid drug release was qualitatively demonstrated although the quantitative calculation of drug release was not obtained in our testing condition.

**In vivo antitumor assay**

**Fig. 6.** The *in vivo* antitumor activity of drug-loaded gels: tumor volumes (A and B), body weights (C and D), and survival rates (E and F) of mice treated with saline, and drug-loaded gels. (L+: light irradiation for 5 min; L-: without light irradiation)

The *in vivo* antitumor efficacy of ROS-responsive gels and control gels was then studied. The typical images of tumor after intratumor injection of various gels were shown in Fig. 3a–3d. Gel formation on the surface of tumors was observed. The gels were then administrated into tumors by intratumor injection and the changes of tumor volume were showed in Fig. 6A. The tumor volume of saline group increased rapidly, suggesting that the saline had no antitumor effect. The groups of G1 and G1<sup>+</sup> showed little inhibition effect, which was probably due to oppression of gel to tumor tissue and thus leading to limited cell apoptosis. The groups of G2 and G2<sup>+</sup> showed obvious tumor suppression effect, demonstrating the efficiency of chemotherapy; the group of G2 shows slightly better antitumor effect than G2<sup>+</sup>, which was due to its ROS-response in ROS-rich tumor tissue environment, resulting in faster gel degradation and more DOX release. The groups of G3(L+) and G3(L+) had obvious antitumor effect, yet G3(L-) and G3(L-) showed little inhibition, indicating the efficiency of photodynamic therapy. More importantly, the group of G4(L+) showed the best antitumor effect and significantly superior to the groups of G2(L-), and G3(L+), suggesting the synergistic effect of chemotherapy and photodynamic therapy. Meanwhile, the groups of G2<sup>+</sup>(L-), G3<sup>+</sup>(L+), and G4(L+) showed comparable antitumor effects, demonstrating that the thioketal containing gelator was the key for the localized chemo-photodynamic therapy. Without thioketal in the backbone of control gels, DOX and ZnPCS<sub>4</sub> cannot efficiently diffuse from the gel network and no synergistic effect was obtained. Taking together, these results demonstrated our hypothesis that the light-triggered ROS-responsive degradation of DOX-ZnPCS<sub>4</sub>-coloaded gel, resulting

into faster release of anticancer drug DOX and photosensitizer ZnPCS<sub>4</sub>, which was also verified in the *in vitro* drug release, and realizing the synergistic effect of localized combined chemophotodynamic therapy.

The systemic toxicity of these gels was also investigated. As shown in Fig. 6C and 6D, negligible weight loss was observed in all groups, except the group of G2\* that showed a maximum 5% weight loss, indicating the low systemic toxicity because of *in situ* gel injection. The survival rates of tumor bearing mice treated with ROS-responsive gels and control gels were supervised and the results were shown in Fig. 6E and 6F, respectively. The groups of saline and G1\* showed no survival after 45 d. The survival rate of group of G1 was 16.7% for 45 d. The mice treated with G2 and G4 with light irradiation showed the best survival rate (80%) for 45 d. The survival rate of group of G4\* was relatively low, indicating the enhanced antitumor effect of ROS-responsive thioketal containing gels. In summary, the combination of chemotherapy and photodynamic therapy effectively improved the antitumor effect and minimized systemic toxicity.

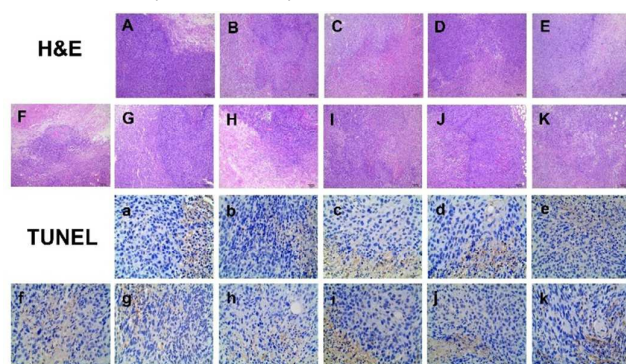


**Fig. 7.** Histological analysis and TUNEL staining of tumors treated with different formulations. A, a: saline(L-); B, b: G1\*(L+); C, c: G2\*(L-); D, d: G3\*(L+); E, e: G3\*(L-); F, f: G4\*(L+); G, g: G1(L+); H, h: G2(L-); I, i: G3(L+); J, j: G3(L-); K, k: G4(L+).

Histological studies were employed to detect the necrosis of cancer cells and induced toxicity.<sup>47,48</sup> The tissue slices of tumor stained with Hematoxylin and eosin (H&E) were presented in Fig. 7, and the other slices of organs stained with H&E were presented in Fig. S8. The group of G4(L+) showed better tumor inhibition effect of 70% tumor necrosis area than other groups. The lungs and livers in all groups had slight inflammatory cell infiltration and the spleens had slight spleen sinus neutrophil infiltration. Besides, the kidneys in all groups were normal in the histological tissue slides. More importantly, there was almost no cardiac toxicity in both experiment and control groups except G4(L+) have a little cardiomyocyte infiltration. These results showed that these formulations showed negligible toxicity to organs. These results also demonstrated that drug-loaded gel administered by intratumor injection could effectively reduce the cardiotoxicity of DOX. The apoptosis of tumor tissue was detected by the terminal deoxynucleotidyl transferase mediated dUTP nick end labeling (TUNEL) assay.<sup>49,50</sup> The group of G4(L+) exhibited the highest apoptotic rate than other groups, demonstrating the best inhibition efficiency (Fig. 7).

## Conclusions

A ROS-responsive injectable low molecular weight gel (LMWG) was fabricated in the mixture solvent of PEG200 and deionized water and showed excellent capacity as a reservoir for anticancer drug and photosensitizer. The ROS-responsive property of thioketal containing gelator was demonstrated by <sup>1</sup>H NMR. The cytotoxicity test and *in vivo* histological analysis showed that the gels had low cytotoxicity and good biocompatibility. The shear thinning and rapidly recovery capability ensured that the gel formation after intratumor injection. The *in vitro* drug release showed that light irradiation triggered the acceleration of drug release in the thioketal containing LWMGs. The ROS-responsive DOX-ZnPCS<sub>4</sub>-co-loaded gel showed the best tumor inhibition and reduced side effects under light irradiation due to the light-triggered cleavage of thioketal bond that resulted in the degradation of gel and release of DOX and ZnPCS<sub>4</sub> for combined chemophotodynamic therapy. Our injectable gel with combined therapy function may provide a platform of engineering localized stimuli-responsive drug delivery system for multimodal therapy.

## Conflicts of interest

There are no conflicts to declare.

## Acknowledgements

The authors thank for the financial support of National Natural Science Foundation of China (No. 51573111, 51773130, 21672164), Program for Changjiang Scholars and Innovative Research Team in University (No. IRT-15R48).

## Notes and references

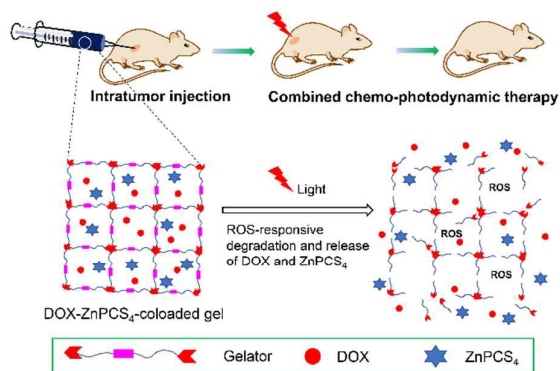
- H. Wang, P. Zhao, W. Su, S. Wang, Z. Liao, R. Niu and J. Chang, *Biomaterials*, 2010, **31**, 8741–8748.
- Q. Chen, C. Li, X. Yang, J. Huang, S. Liu, W. Liu, J. Liu and K. Wang, *J. Mater. Chem. B*, 2017, **5**, 7529–7537.
- C. K. Chen, W. C. Law, R. Aalinkeel, Y. Yu, B. Nair, J. Wu, S. Mahajan, J. L. Reynolds, Y. Li, C. K. Lai, E. S. Tzanakakis, S. A. Schwartz, P. N. Prasad and C. Cheng, *Nanoscale*, 2014, **6**, 1567–1572.
- Y. Wang, G. Guo, Y. Feng, H. Long, D.-L. Ma, C.-H. Leung, L. Dong and C. Wang, *J. Mater. Chem. B*, 2017, **5**, 7307–7318.
- Z. Xu, K. Zhang, C. Hou, D. Wang, X. Liu, X. Guan, X. Zhang and H. Zhang, *J. Mater. Chem. B*, 2014, **2**, 3433–3437.
- S. A. Senevirathne, K. E. Washington, M. C. Biewer and M. C. Stefan, *J. Mater. Chem. B*, 2016, **4**, 360–370.
- S. A. Senevirathne, K. E. Washington, J. B. Miller, M. C. Biewer, D. Oupicky, D. J. Siegwart and M. C. Stefan, *J. Mater. Chem. B. Mater. Bio. Med*, 2017, **5**, 2106–2114.
- J. Fang, H. Nakamura and H. Maeda, *Adv. Drug Deliv. Rev.*, 2011, **63**, 136–151.
- Y. Pu, S. Chang, H. Yuan, G. Wang, B. He, Z. Gu, *Biomaterials*, 2013, **34**, 3658–3666.

## ARTICLE

## Journal Name

- 10 M. Norouzi, B. Nazari and D. W. Miller, *Drug Discov. Today*, 2016, **21**, 1835–1849.
- 11 M. He, J. Sui, Y. Chen, S. Bian, Y. Cui, C. Zhou, Y. Sun, J. Liang, Y. Fan and X. Zhang, *J. Mater. Chem. B*, 2017, **5**, 4852–4862.
- 12 X. Chen, P. Yuan, Z. Liu, Y. Bai and Y. Zhou, *J. Mater. Chem. B*, 2017, **5**, 5968–5973.
- 13 M. S. Gil, T. Thambi, V. H. G. Phan, S. H. Kim and D. S. Lee, *J. Mater. Chem. B*, 2017, **5**, 7140–7152.
- 14 C. Wang, X. Wang, K. Dong, J. Luo, Q. Zhang and Y. Cheng, *Biomaterials*, 2016, **104**, 129–137.
- 15 W. Zhang, X. Zhou, T. Liu, D. Ma and W. Xue, *J. Mater. Chem. B*, 2015, **3**, 2127–2136.
- 16 H. Kuang, H. He, Z. Zhang, Y. Qi, Z. Xie, X. Jing and Y. Huang, *J. Mater. Chem. B*, 2014, **2**, 659–667.
- 17 R. Tian, J. Chen and R. Niu, *Nanoscale*, 2014, **6**, 3474–3482.
- 18 Y. Hu, W. Gao, F. Wu, H. Wu, B. He and J. He, *J. Mater. Chem. B*, 2016, **4**, 3504–3508.
- 19 L. Latxague, M. A. Ramin, A. Appavoo, P. Berto, M. Maisani, C. Ehret, O. Chassande and P. Barthelemy, *Angew. Chem. Int. Ed.*, 2015, **54**, 4517–4521.
- 20 M. T. McClendon and S. I. Stupp, *Biomaterials*, 2012, **33**, 5713–5722.
- 21 K. H. Bae, L.-S. Wang and M. Kurisawa, *J. Mater. Chem. B*, 2013, **1**, 5371–5388.
- 22 M. Singh, S. Kundu, M. A. Reddy, V. Sreekanth, R. K. Motiani, S. Sengupta, A. Srivastava and A. Bajaj, *Nanoscale*, 2014, **6**, 12849–12855.
- 23 D. Mandal, S. K. Mandal, M. Ghosh and P. K. Das, *Chemistry*, 2015, **21**, 12042–12052.
- 24 M. A. Ramin, K. R. Sindhu, A. Appavoo, K. Oumzil, M. W. Grinstaff, O. Chassande and P. Barthelemy, *Adv. Mater.*, DOI: 10.1002/adma.201605227.
- 25 W. Gao, Y. Liang, X. Peng, Y. Hu, L. Zhang, H. Wu and B. He, *Biomaterials*, 2016, **105**, 1–11.
- 26 L. Xu, Y. Liang, C. Sun, N. Hao, J. Yan, W. Gao and B. He, *Nanotheranostics*, 2017, **1**, 313–325.
- 27 L. Pan, Y. Li, L. Zhu, B. Zhang, Y. Shen and A. Xie, *Mater. Sci. Eng. C*, 2017, **75**, 1448–1455.
- 28 M. Lee, H. Lee, N. Vijayakameswara Rao, H. S. Han, S. Jeon, J. Jeon, S. Lee, S. Kwon, Y. D. Suh and J. H. Park, *J. Mater. Chem. B*, 2017, **5**, 7319–7327.
- 29 A. R. Karimi, A. Khodadadi and M. Hadizadeh, *RSC Adv.*, 2016, **6**, 91445–91452.
- 30 X. Deng, Y. Liang, X. Peng, T. Su, S. Luo, J. Cao, Z. Gu and B. He, *Chem. Commun.*, 2015, **51**, 4271–4274.
- 31 K. Han, W.-Y. Zhang, J. Zhang, Q. Lei, S.-B. Wang, J.-W. Liu, X.-Z. Zhang and H.-Y. Han, *Adv. Funct. Mater.*, 2016, **26**, 4351–4361.
- 32 Y. T. Chiang, Y. W. Yen and C. L. Lo, *Biomaterials*, 2015, **61**, 150–161.
- 33 J. J. Hu, Q. Lei, M. Y. Peng, D. W. Zheng, Y. X. Chen and X. Z. Zhang, *Biomaterials*, 2017, **128**, 136–146.
- 34 T. Wang, D. Wang, J. Liu, B. Feng, F. Zhou, H. Zhang, L. Zhou, Q. Yin, Z. Zhang, Z. Cao, H. Yu and Y. Li, *Nano Lett.*, 2017, **17**, 5429–5436.
- 35 D. S. Wilson, G. Dalmaso, L. Wang, S. V. Sitaraman, D. Merlin and N. Murthy, *Nat. Mater.*, 2010, **138**, 923–928.
- 36 J. Wang, X. Sun, W. Mao, W. Sun, J. Tang, M. Sui, Y. Shen and Z. Gu, *Adv. Mater.*, 2013, **25**, 3670–3676.
- 37 H. Zhang, X. Zhu, Y. Ji, X. Jiao, Q. Chen, L. Hou, H. Zhang and Z. Zhang, *J. Mater. Chem. B*, 2015, **3**, 6310–6326.
- 38 F. Song, L.-M. Zhang, J.-F. Shi, N.-N. Li, C. Yang and L. Yan, *Mater. Sci. Eng. C*, 2010, **30**, 804–811.
- 39 S. Pan, S. Luo, S. Li, Y. Lai, Y. Geng, B. He and Z. Gu, *Chem. Commun.*, 2013, **49**, 8045–8047.
- 40 D. V. Nguyen, F. Li, H. Li, B. S. Wong, C. Y. Low, X. Y. Liu and L. Kang, *Mol. Pharm.*, 2015, **12**, 444–452.
- 41 M. K. Gupta, J. R. Martin, T. A. Werfel, T. Shen, J. M. Page and C. L. Duvall, *J. Am. Chem. Soc.*, 2014, **136**, 14896–14902.
- 42 Liu, D. Wang, Y. Liu, Q. Zhang, L. Meng, H. Chi, J. Shi, G. Li, J. Li and X. Zhu, *Polym. Chem.*, 2015, **6**, 3460–3471.
- 43 C. Yue, C. Zhang, G. Alfranca, Y. Yang, X. Jiang, Y. Yang, F. Pan, J. M. de la Fuente and D. Cui, *Theranostics*, 2016, **6**, 456–469.
- 44 H. Wu, S. Liu, L. Xiao, X. Dong, Q. Lu and D. L. Kaplan, *ACS Appl. Mater. Interfaces*, 2016, **8**, 17118–17126.
- 45 X. Yan, Q. Chen, L. Zhu, H. Chen, D. Wei, F. Chen, Z. Tang, J. Yang and J. Zheng, *J. Mater. Chem. B*, DOI: 10.1039/c7tb01780d.
- 46 L. Aulisa, H. Dong and J. D. Hartgerink, *Biomacromolecules*, 2009, **10**, 2694–2698.
- 47 Z. Duan, Y. Zhang, H. Zhu, L. Sun, H. Cai, B. Li, Q. Gong, Z. Gu and K. Luo, *ACS Appl. Mater. Interfaces*, 2017, **9**, 3474–3486.
- 48 Y. Liang, X. Deng, L. Zhang, X. Peng, W. Gao, J. Cao, Z. Gu and B. He, *Biomaterials*, 2015, **71**, 1–10.
- 49 Y. Liang, W. Gao, X. Peng, X. Deng, C. Sun, H. Wu and B. He, *Biomaterials*, 2016, **100**, 76–90.
- 50 W. She, N. Li, K. Luo, C. Guo, G. Wang, Y. Geng and Z. Gu, *Biomaterials*, 2013, **34**, 2252–2264.

## Table of Content



A ROS-responsive low molecular weight hydrogel was fabricated and loaded with anticancer drug and photosensitizer for efficient chemo-photodynamic therapy.